

Early Consideration on an Active Mitigation System for CubeSat Reaction Wheels Magnetic Field

Anargyros T. Baklezos, Theodoros N. Kapetanakis, Ioannis O. Vardiambasis and Christos D. Nikolopoulos
Hellenic Mediterranean University, 3, Romanou str., Chania, 73133, Greece,



EEITE 2022

3RD INTERNATIONAL CONFERENCE IN ELECTRONIC ENGINEERING, INFORMATION TECHNOLOGY & EDUCATION

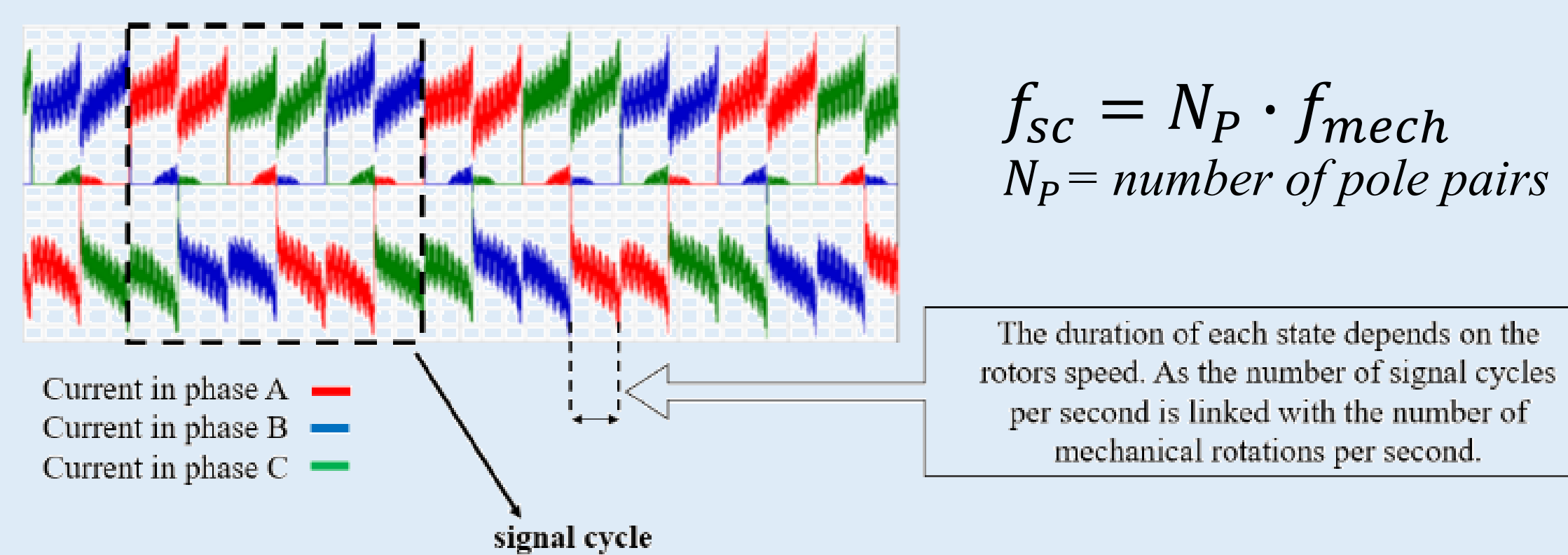
1. Introduction

The rapid growth in small satellite operations and their applications lead to the introduction of more complex systems due to their miniaturization of electronics, circuits and sensors. Regarding EMC aspect, one of the main features that most science mission should comply to is the magnetic cleanliness in the area of sensitive equipment. Reaction wheel components such as the electric motor and various ferromagnetic parts at high-speed operation result in significant electromagnetic stray fields in various frequency ranges. Main approach to overcome this issue is to provide additional magnetic shielding to the attitude control subsystem that has an impact on the total weight of the microsatellite. Another mitigation strategy is placing the sensitive equipment as far as possible from the radiating sources, but this has no application in the small satellites structures (MicroSats, CubeSats, etc). Numerous studies towards this direction have been done in the past, but nowadays other mitigation techniques are proposed that virtually try to minimize the magnetic fields on sensitive satellite areas. The knowledge of the magnetic behavior of the RWA can actively cancel the interference at any given area by generating an opposite magnetic field. Thus, knowing the exact voltage driven RWA behavior, an engineer can easily adjust the mapping between the produced interference and the current of the “canceling” source’s magnetic field.

Magnetic field generation

Multiple magnet pairs and wire windings are used in the rotor and stator respectively to achieve smooth torque output. The magnetic field emissions of a rotating Brushless DC (BLDC) Motor can be attributed to two sources, rotating a bunch of permanent magnets (i.e. the rotor) with a certain frequency which will produce a spectral component at the frequency (f_{mech}) of the mechanical rotation, and powering the three phases of the stator in order to create the rotating magnetic field which turns the rotor. For a three phase BLDC motor with a sensorless driving scheme (driven without Hall sensors, using the back EMF instead), at each state two phases are powered (opposite to one another) while the third is used as an input by the Speed Controller to identify the correct moment for state transition. That’s the reason why BLDC motors driven sensorlessly cannot operate at very low speeds (lower than 1300 rpm approximately for our case), as an adequate speed is required for a large enough back EMF voltage to be induced to the coil of the “sensing phase”.

The process described above (at each state 2 opposite powered phases) produces 6 possible combinations for the current in the stator coils. The sequence of those 6 states comprises a signal cycle (electrical cycle).



Typical BLDC motors used in RC cars or drones have 14-16 poles to achieve large mechanical torque while minimizing the required current. Our motors have 14 poles, therefore 7 pole pairs. The number of signal cycles per second (for the current powering the stator’s phases) can be obtained by multiplying the f_{mech} with the number of pole pairs on the rotor. Therefore, these currents’ digital waveforms have a fundamental frequency of f_{sc} , producing emissions at f_{sc} and its harmonics

References

- [1] A. Nicolai, S. Stoltz, L. Hafemeister, S. Scheiding, O. Hillenmaier, and C. Strauch, “The Magnetically Clean Reaction Wheel: Results and Performance,” in *2022 ESA Workshop on Aerospace EMC (Aerospace EMC)*, 2022, pp. 1–7. doi: 10.23919/AerospaceEMC54301.2022.9828554.
- [2] A. Nicolai *et al.*, “Towards a Magnetically Clean Reaction Wheel with Active Magnetic Field Mitigation,” in *2019 ESA Workshop on Aerospace EMC (Aerospace EMC)*, 2019, pp. 1–6. doi: 10.23919/AeroEMC.2019.8788947.
- [3] V. Pronenko, S. Belyayev, and F. Dudkin, “Electromagnetic compatibility analysis for small satellites: Method and instrumentation,” 2016. doi: 10.1109/MetroAeroSpace.2016.7573182.
- [4] M. D. Michelena, A. A. O. Cencerrado, J. De Frutos Hermansanz, and M. Á. R. Rodríguez, “New Techniques of Magnetic Cleanliness for Present and Near Future Missions,” 2019. doi: 10.1109/EMCEurope.2019.8872024.
- [5] C. D. Nikolopoulos, A. T. Baklezos, and C. N. Capsalis, “On Achieving Spacecraft Level Magnetic Cleanliness with Proper Equipment Ordinance of DC and ELF Magnetic Sources,” *IEEE Trans. Electromagn. Compat.*, vol. 62, no. 6, pp. 2714–2724, May 2020, doi: 10.1109/TEMC.2020.2992682.
- [6] P. Narvaez, “The magnetostatic cleanliness program for the Cassini spacecraft,” *Space Sci. Rev.*, 2004, doi: 10.1007/s11214-004-1433-1.

The first step on creating an active system capable of cancelling the emissions of the RWA at a certain point, is the accurate modeling of the motor’s emissions. For this reason, a plane passing from the center of the motor is defined, while it is parallel to the plane incident to the motor’s base. This plane is in $x - y$ as depicted in the following Figure:

$$i_n = -\sin(\theta) \cdot i_x + \cos(\theta) \cdot i_z$$

$$m_1 = m_1 \cdot i_n$$

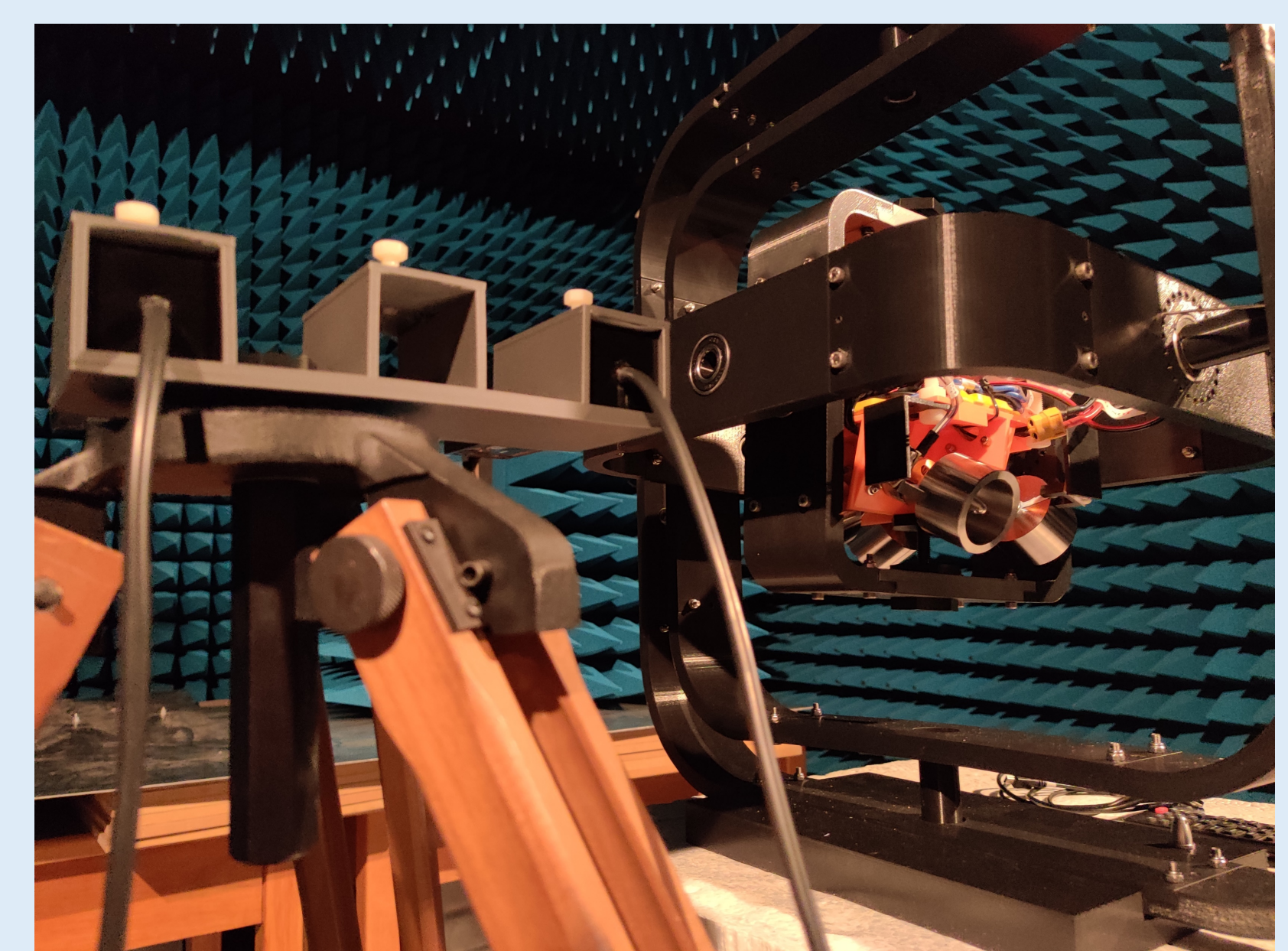
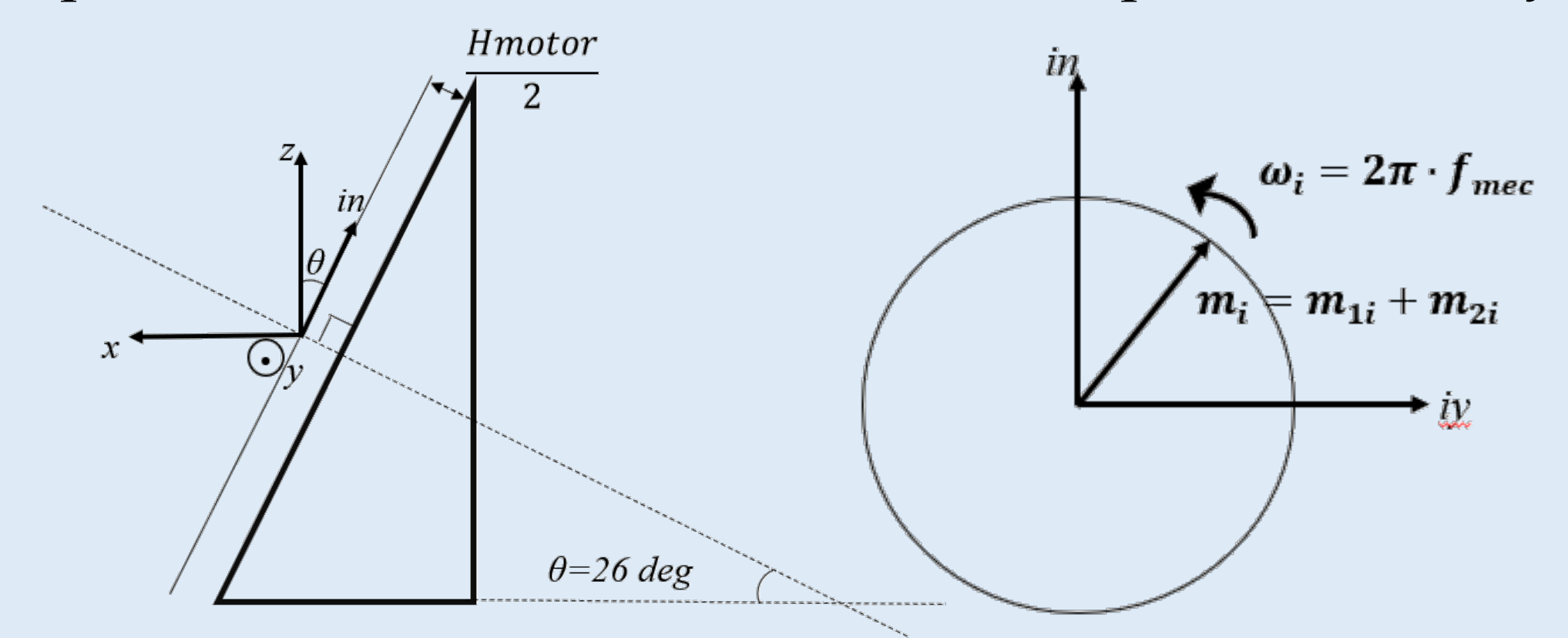
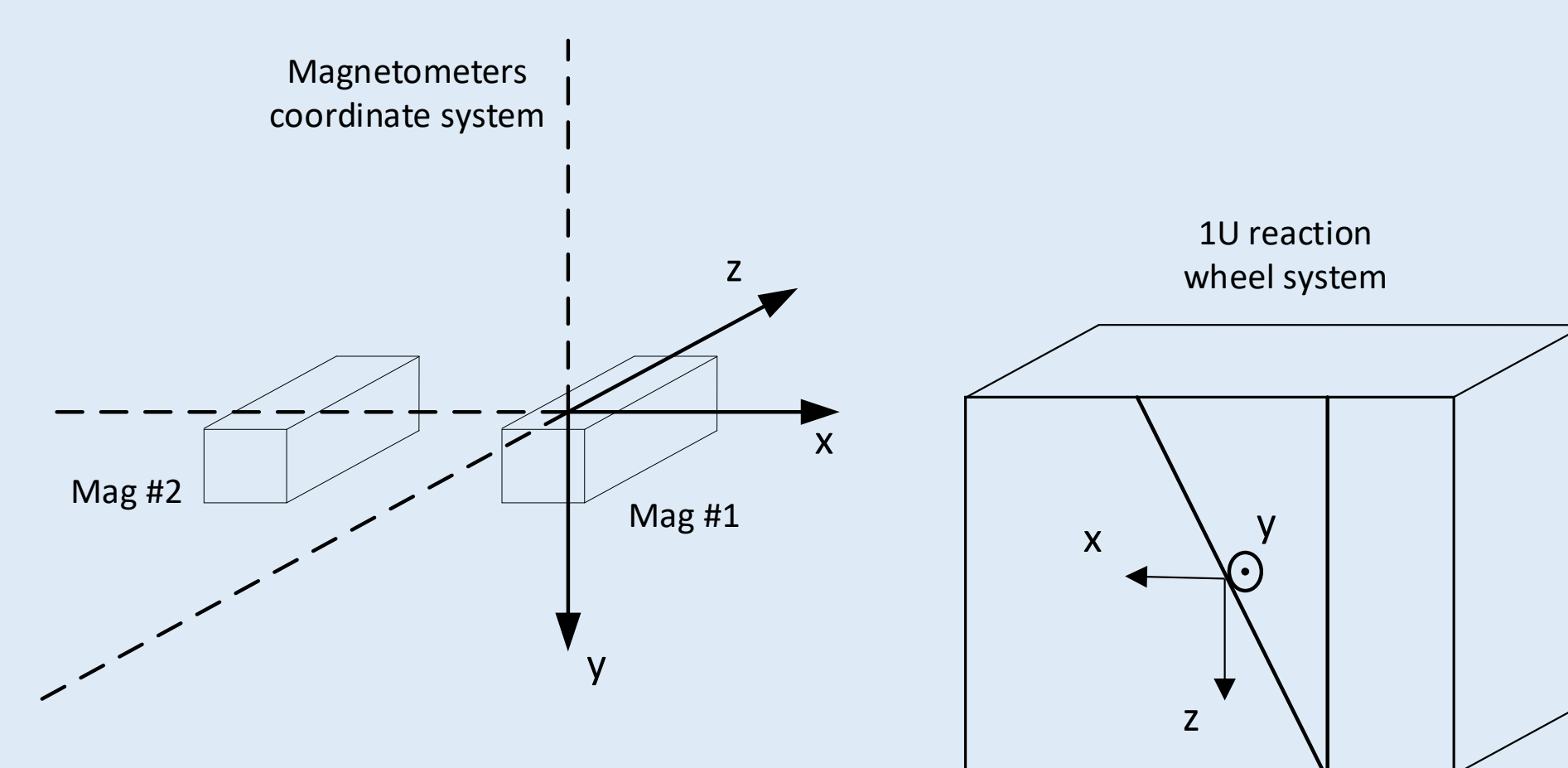
$$m_2 = m_2 \cdot i_y$$

$$m_{1i=1:14} = A \cdot \sin(2\pi \cdot f_{mec} \cdot t + (i-1) \cdot 25.714)$$

$$m_{2i=1:14} = A \cdot \cos(2\pi \cdot f_{mec} \cdot t + (i-1) \cdot 25.714)$$

2. Measurement Setup

In order to evaluate the real time contribution of the 4-reaction wheel system, the measurement layout depicted in the figure below has been implemented. Two fluxgate magnetometers have been placed perpendicular to the 1U (CubeSat-like) structure which is embedded in a gimbal arrangement in order to be able for a 3-D movement.



For each magnetic dipole, where the first magnetometer is at the distance vector $R=(0.263m, -0.0335m, -0.03m)$ and simplifying the equations due to quasi-static approach:

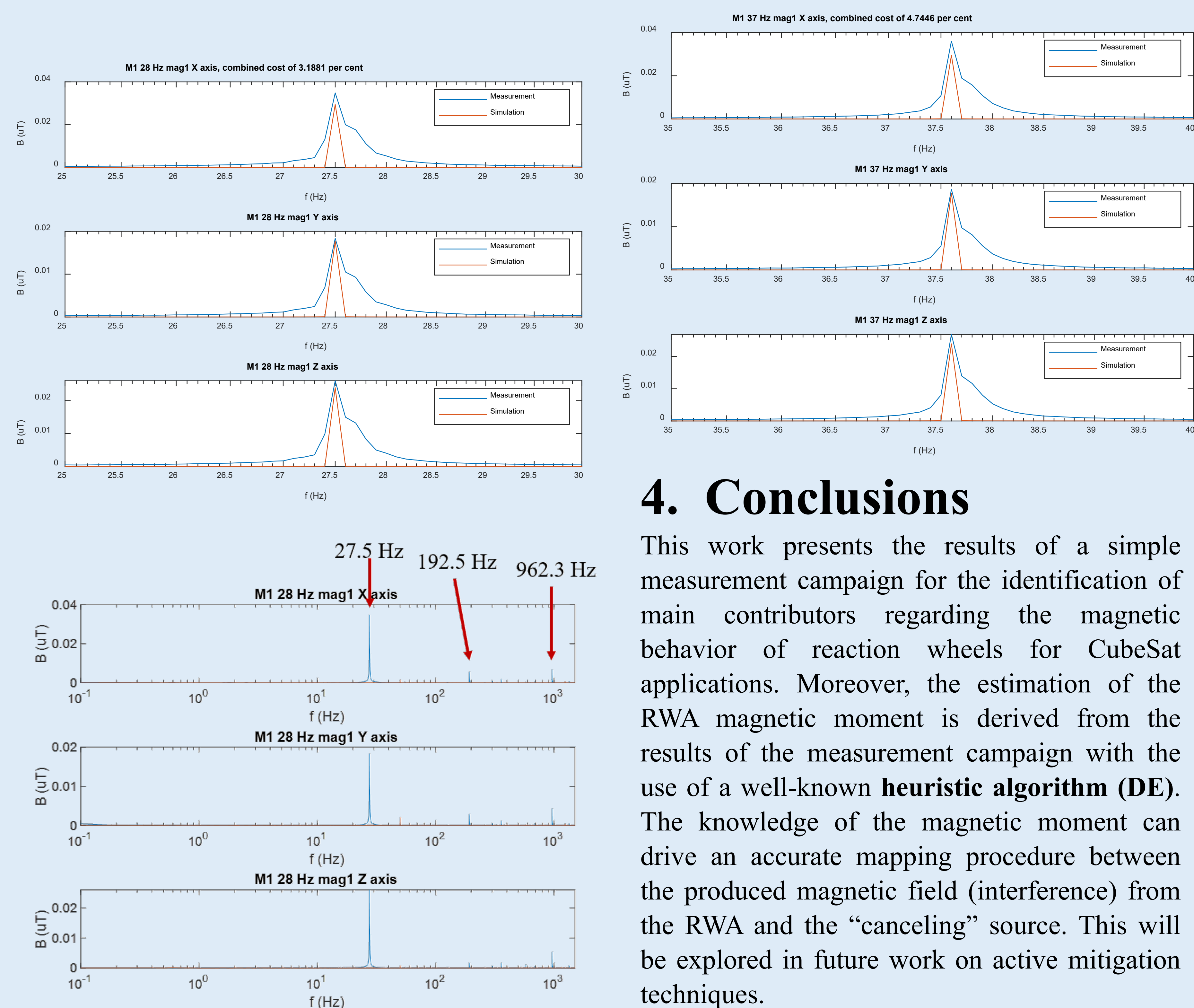
$$H_{1i} = \frac{3 \cdot m_{1i} \cdot (i_n \cdot i_R) \cdot i_R - m_{1i} \cdot i_n}{4 \cdot \pi \cdot R^3}$$

$$H_{2i} = \frac{3 \cdot m_{2i} \cdot (i_y \cdot i_R) \cdot i_R - m_{2i} \cdot i_y}{4 \cdot \pi \cdot R^3}$$

$$B = \mu_0 \cdot \sum_{i=1}^{14} (H_{1i} + H_{2i})$$

3. Results

The following figures depict the results of the measured magnetic behavior of one reaction wheel (motor1) in order to calculate its magnetic moment (source of interference) for different frequencies f_{mech}



4. Conclusions

This work presents the results of a simple measurement campaign for the identification of main contributors regarding the magnetic behavior of reaction wheels for CubeSat applications. Moreover, the estimation of the RWA magnetic moment is derived from the results of the measurement campaign with the use of a well-known heuristic algorithm (DE). The knowledge of the magnetic moment can drive an accurate mapping procedure between the produced magnetic field (interference) from the RWA and the “canceling” source. This will be explored in future work on active mitigation techniques.